Article

Long Wavelength SAR Backscatter Modelling Trends as a Consequence of the Emergent Properties of Tree Populations

Matthew Brolly [1,2,]* and Iain H. Woodhouse [3]

[1] School of Environment and Technology, University of Brighton, Cockcroft Building, Lewes Road, Brighton BN2 4GJ, UK

[2] Department of Geographical Sciences, University of Maryland, College Park, MD 20742, USA

[3] School of GeoSciences, The University of Edinburgh, Drummond Street, Edinburgh EH8 9XP, UK; E-Mail: I.H.Woodhouse@ed.ac.uk

* Author to whom correspondence should be addressed; E-Mail: M.Brolly@Brighton.ac.uk; Tel.: +44-1273-642-282.

Abstract: This study describes the novel use of a macroecological plant and forest structure model in conjunction with a Radiative Transfer (RT) model to better understand interactions between microwaves and forest canopies. Trends predicted by the RT model, resulting from interactions with mixed age, mono and multi species forests, are analysed in comparison to those predicted using a simplistic structure based scattering model. This model relates backscatter to scatterer cross sectional or volume specifications, dependent on the size. The Spatially Explicit Reiterative Algorithm (SERA) model is used to provide a widely varied tree size distribution while maintaining allometric consistency to produce a natural-like forest representation. The RT model is parameterised using structural information from SERA and microwave backscatter simulations are used to analyse the impact of changes to the forest stand. Results show that the slope of the saturation curve observed in the Synthetic Aperture Radar (SAR) backscatter-biomass relationship is sensitive to thinning and therefore forest basal area. Due to similarities displayed between the results of the RT and simplistic model, it is determined that forest SAR backscatter behaviour at long microwave wavelengths may be described generally using equations related to total stem volume and basal area. The nature of these equations is such that they describe saturating behaviour of forests in the absence of attenuation in comparable fashion to the trends exhibited using the RT model. Both modelled backscatter trends predict a

relationship to forest basal area from an early age when forest volume is increasing. When this is not the case, it is assumed to be a result of attenuation of the dominant stem-ground interaction due to the presence of excessive numbers of stems. This work shows how forest growth models can be successfully incorporated into existing independent scattering models and reveals, through the RT comparison with simplistic backscatter calculations, that saturation need not solely be a direct result of attenuation.

1. Introduction

The effective exploitation of airborne and spaceborne Synthetic Aperture Radar (SAR) for modern forestry applications relies on sound theoretical understanding of the relationship between backscatter and generalised forest parameters such as volume and/or biomass. The "Water Cloud Model" (WCM) [1] and "Random Volume over Ground" (RVoG) [2] have become two of the most widely used simplifications of microwave scattering from forests. The models have a substantial heritage of being applied to solve both incoherent and coherent observations over forested areas. A consequence of both models is that the saturation of backscatter with increasing forest biomass can only be explained as a result of the increasing attenuating properties of forest canopies; *i.e.*, saturation occurs when the forest layer effectively becomes opaque. However, there is both theoretical [3] and empirical [4,5] evidence showing that in certain conditions saturation can occur at lower biomass than expected and sometimes saturation does not occur at all, suggesting that the WCM and RVoG models may not be as generally applicable as is widely thought. In particular, saturation may be caused by other factors, such as the ratio of dominant stem radius to wavelength [6–8].

Woodhouse [3] initially demonstrated how macroecology could be used to aid the process of simplifying forest structure for forward modelling in remote sensing. The model used was the "General model for structure and allometry of plant vascular systems" (WBE) [9], which has its roots in an explanation for the origin of allometric scaling laws. Despite some important limitations this model displays key advantages that make it an appropriate first-order linkage between simple backscatter modelling and models of biological function, effectively shown in Brolly and Woodhouse [10]. WBE is based on the constraints of biomechanics and resource distribution for a single plant. Spatially Explicit Reiterative Algorithm (SERA) on the other hand, is an area-based model that has similar macroecological principles imbedded, but uses them to model plant (tree) communities [11,12]. It achieves this by accounting for light and space competition as SERA, by design, evaluates how "different species compete in a world space whose physical attributes are clearly defined".

In this work the SERA description of forest population structure from a single run is used as input to a radiative transfer model, RT2, to simulate radar (microwave) backscatter values expected from airborne or spaceborne SAR imagers [13]. The Radiative Transfer (RT2) model has been used in a similar manner in, for example [8,10,14].

By modelling backscatter in this way the aim of this study was primarily to examine the feasibility of bringing two independent models together to seek new generalised insight into forest backscatter saturation behaviour relating to area-based forest structural variations within a multi-age forest. The purpose was to examine whether backscatter-biomass trends are solely the consequence of increased obstruction of deeper layers of the forest, as is widely assumed, or can be explained by generic structural properties of a population of trees. Specifically this will be done by relating backscatter values to forest parameters using the definitions of radar scattering outlined in Crispin and Maffett [15]. This will provide the basis of the simplistic model which assumes a proportional relationship between backscatter and cross-sectional area when the radii of all the stems are large enough for complete Optical scattering, and a proportional relationship between backscatter and volume squared when they are small enough for complete Rayleigh scattering. These ideas are introduced more completely in Section 2.2. Modelling backscatter from modelled forest populations allows every aspect of the forest to be compared with radar backscatter behaviour generated from both RT2 and a simplified model specifically relating backscatter to total basal area and volume. The influence of not only biomass variations but in particular stem number densities, and stand basal areas can be readily assessed using a forest framework that adds extra complexity to the analysis offered previously by theoretical models such as the so-called "Matchstick Model" [8].

In a similar way to the WCM and the RVoG models, the forest model used in this study is a broad simplification of forest structure. All three models assume that the canopy can be characterised by a small number of representative scatterers. For the WCM these are identical spherical scatterers; for RVoG these are identical randomly oriented cylinders; for the Matchstick model they are randomly oriented identical cylinders but of varying size and number density as governed by realistic limits of general macroecological relationships [3]. Theoretically, these three models are optimum for different radar wavelengths: WCM for short wavelengths, such as C-band, RVoG for L-band, and the Matchstick Model for long wavelengths, such as P-band and Very High Frequency (VHF). In the current study we only consider long wavelength SAR simulations and so make an assumption that the stem scattering dominates the overall trend [16] through both direct stem and ground-stem interactions. In addition to the structural limitations the use of radiative transfer models for modelling absolute radar backscatter values has been shown in the literature to become less reliable at long wavelengths due to the modelling of the electromagnetic field as being incoherent and the increasing significance of coherent scattering interactions (e.g., double bounce) associated with forest scattering at such wavelengths. The extent of this limitation is outlined in Saatchi and McDonald [17] where radiative transfer (incoherent) and distorted born (coherent) scattering models are compared. At low frequencies the models do not produce equivalent results due to the absence of coherent summation in radiative transfer models. At P-Band frequencies and lower, as well as in sparse forest canopies, this scattering mechanism is of particular significance with, in many cases, the double bounce scattering dominating. The discrepancy in absolute terms resulting from this limitation is shown in Saatchi and McDonald [17] to be in the order of up to 3 dB for all polarisations with the radiative transfer model generally underestimating radar backscatter. The effect is most prevalent when considering crown-ground interactions (this scattering mechanism is not considered in this study). As a consequence, in this study the backscatter trends, rather than absolute values, are the most significant aspect of the presented results, with the discrepancy in absolute terms noted as a limitation of the study for direct comparison to real data. This

study does not attempt to validate backscatter predictions but rather reinforces the ideas concerning the exhibited trends and similarities exhibited between the predictions made by the radiative transfer model and the simplistic model independently.

2. Methods

2.1. Spatially Explicit Reiterative Algorithm (SERA)

SERA is a forest growth model which accurately reproduces the community dynamics of a collection of trees competing for light and space resources. According to Enquist *et al*. [18] a variety of plant ensembles are observed to "self-thin" in accord with the same or very similar scaling exponents to one another. As a result of this, Spatially Explicit Reiterative Algorithm (SERA) was designed to incorporate this self-management technique to allow evaluation of how different species compete when the physical attributes, such as the direction and intensity of incident sunlight, are clearly defined. SERA provides a first estimate of the outcome of forest dynamics in a homogeneous environment from the onset of plantation until a user-defined point. Variability of water and nutrient resources is not considered.

Within SERA each plant is intentionally simplified to consist of a single photosynthetic surface elevated by a single stem. Similar concepts have been explored in [19–21] but in this work the canopy is only used to determine ensemble growth. Whereas some models represent the canopy as a flat disc, SERA treats each canopy as a hemispheric layer of uniform thickness (flat discs overestimate the ability of a tree to capture light and shade others). The angle of solar incidence is time averaged to 0 degrees such that the projected canopy area is the total photosynthetic area available for each plant. For the purpose of the backscatter modelling, we consider only longer wavelengths and therefore do not include the canopy. The choice to not model canopy interactions is taken both because of the lack of branching architecture provided by the SERA canopy design and also to allow specific investigations relating to the Matchstick Model of Brolly and Woodhouse [8] that models stem backscatter at long wavelengths where canopy contributions have negligible influence on trends. The minimal sensitivity and extinction within this region of long microwaves further validates this choice. While this is an appropriate assumption for very long wavelengths (*i.e.*, VHF where attenuation from foliage is minimal and stems dominate the backscatter [22]) it is less valid when attenuation from foliage becomes significant (*i.e.*, L-band and shorter ([23,24]). In these studies it is stated that scattering and attenuation by foliage scales with frequency so that the majority of backscatter originates from interactions with the foliage level of the forest at C-Band, the branches at L-Band, and the trunks and ground at P-Band and longer. Praks *et al*. [25] provide an example of how foliage attenuation influences scattering phase centre heights using SAR interferometry. Signal penetration to the canopy floor is more common when using longer wavelengths due to a reduction of this attenuation. In Praks *et al*. [25] the forest height estimate for X-Band is 25% lower than the laser derived tree top line while at L-Band this height is located at a value closer to 50% of the laser derived value. The proportion of energy transmitted to the ground is in general an indicator of the level of attenuation, with more ground contribution suggesting less attenuation and lower height estimates. A further example is seen for P and L Bands in Papathanassiou *et al*. [26].

One of the advantages of SERA is that it requires relatively few input variables, consisting of 20 species-specific parameters and representative values. Of these variables only six scaling exponents are required to generate a species. Unlike WBE, the relationships in SERA that govern allocation of stem mass to stem diameter and height allow a transition from stem geometric self-similarity to geometric non-similarity. Such considerations were given in Woodhouse [3]. SERA also allows scaling exponents to change within the lifetime of a stem with the scaling change found empirically to occur around the onset of maturity. SERA also minimises input parameters by assuming species similarities [27,28].

SERA consistently predicts that plant lifetimes scale as the one-quarter power of body mass, a scaling relationship that has been reported for diverse plant species [29]. A number of naturally occurring scaling relationships also emerge as the direct result of competition for light and space, even in a simple homogeneous scenario. Many of the scaling relationships predicted by SERA also emerge from WBE suggesting that SERA and other mathematical/theoretical explanations for observed real-world scaling relationships have conceptual common ground. When plants violate physical laws, such as the Euler-Greenhill mechanical relationship governing the buckling height of a stem [30], the result is death. Mortality also results from light deprivation or stochastic/age-dependent processes. In this way SERA's "self-thinning" closely replicates empirical trends.

SERA's robustness was assessed biologically through comparison with the ensemble behaviour of thoroughly investigated and collated empirical data. The worldwide compendium for forestry data compiled by Cannell [31] was used as a reference to survey the primary literature published before 1982 to identify long term studies of monospecific forests. Of these the most useful data set for any species was for a single *Abies alba* population documented every 5 years for 95 years starting 10 years after initial planting (referenced and used in Hammond and Niklas [12]). The Cannell [31] dataset was then used to statistically characterise 332 angiosperm and 343 conifer dominated communities to emulate the dynamics of "generalised" populations.

The high extent to which SERA was successful at emulating the behaviour of real forest populations is documented in Hammond and Niklas [12]. The true capability of SERA is its ability to predict the fate of a species under varying degrees of spatial and temporal heterogeneity. Figure 1 emphasises the visual capabilities of SERA when presenting the evolution of a randomly seeded forest.

2.2. Rayleigh and Optical Scattering

In Brolly and Woodhouse [8,10] it was shown that it is possible to make a first order estimate of trends of backscatter using some approximations based on whether the stem cylinders lie in the Rayleigh or Optical scattering domain. In a similar fashion the trends in backscatter as a function of stem radius were considered. The three possibilities for a multi age and multi species forest that exist are: (1) the stem specifications lie completely in the Rayleigh scattering domain; (2) they lie entirely in the domain of Optical scattering; and (3) the stems consist of both size classes spanning both domains. In the Rayleigh case we assume the backscatter from each cylinder increases with the square of the volume, and for Optical, it increases with the physical cross-section [32]. At the transition between these two regimes Mie scattering is dominant but an approximation is made that assumes resonant behaviour of Mie "averages out" across this region giving the cumulative effect of a distribution of stem sizes. This assumption is supported by multi frequency empirical results, for example see

Lopes *et al.* [33] and Mougin *et al.* [34]. As a means of detailed modelling of forest backscatter this is a major simplification, but in terms of characterising the backscatter using representational scatterers (as is the case in the WCM and RVoG) we consider it appropriate.

Figure 1. Horizontal and bottom-up representation of *Abies alba* forest emanating from single stem. Snapshots at (**a**) 40, (**b**) 60, (**c**) 80, and (**d**) 100 years. Width of plots are 100 m. Brown represents stems, darkness of green represents level of canopy shading (*i.e.*, bright green represents unshaded canopy). Blue represents sky, indicating zero canopy cover between ground and sky. Young plots are not included as sexual maturity is required to replicate.

| (a) | (b) | (c) | (d) |
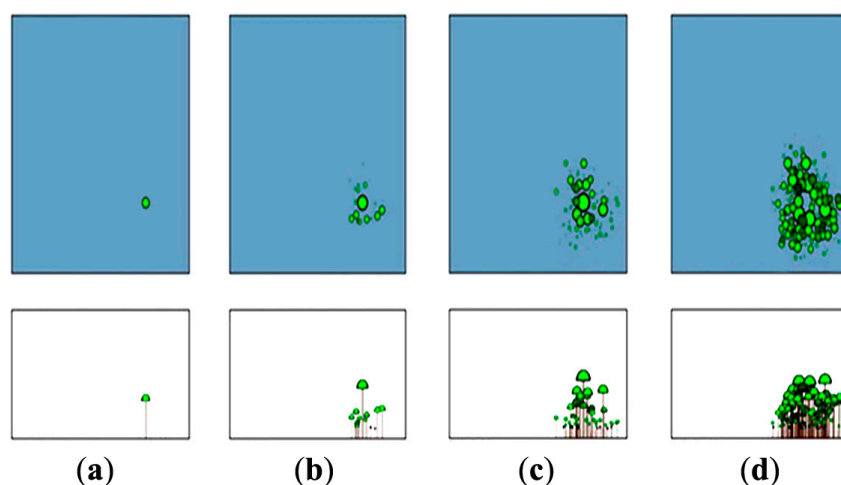
Using the data provided by SERA the forest can be segregated according to whether the stems are expected to scatter in the Optical or Rayleigh regimes and the corresponding backscatter generated accordingly.

For Rayleigh scattering, the total radar cross-section (RCS) of the collection of N stems, is given by a proportionality to the square of the stem volume (V^2) multiplied by the number of stems within the stand (N) ([6,35]):

$$\sigma_{Rayleigh} \propto N\,V^2 \tag{1}$$

Due to the nature of this scattering the maximum backscatter will originate from the largest stems with size dominating over number density when all stems are Rayleigh scatterers [8].

In a similar manner, the scenario whereby the radii of all the stems are large enough for the cylinders to lie completely in the Optical region can be considered. In this case the RCS of the stand scales with the physical cross-section or total basal area according to the relationship between geometric and physical optics as published in Hestilow [36] and evident under particular scaling properties of the scatterer with the physical and geometric optics solutions corresponding when scaling follows particular conditions:

$$\sigma_{Optical} \propto N\,A \tag{2}$$

where N is the number of stems and A the cross sectional area.

The ratio of radius (r) to incident wavelength (λ) governs the nature of scattering. For this work the limits are determined by

$$2\,\pi r > 0.1\,\lambda \tag{3}$$

for the Rayleigh-Mie boundary, and

$$2\,\pi r < 10\,\lambda \tag{4}$$

for the Mie-Optical boundary respectively. These limits are the same as those outlined in Woodhouse [35] and Moosmuller and Arnott [32]. In this work, we assume the Mie scattering is averaged out over a range of radii, so that Mie scattering is approximated as Optical scattering [15].

If the backscatter is solely generated by Optical scattering then as the number of stems reduces the backscatter will decrease, but as the size of the remaining stems increase the backscatter will do so also. Therefore a scenario must exist whereby the reduction in numbers and the increase of the largest stems would result in equilibrium and therefore backscatter "saturation" would be predicted.

3. Modelling Strategy

By coupling the SERA model to radiative transfer theory and ideas applying to the approach set out in the Matchstick Model [8] only one layer of scatterers describing the stem properties is required. The limits of this layer are defined by the height of the tallest stem present at any time, and the ground surface, a typical consideration for longer microwave wavelengths. The radiative transfer model used here is RT2, a multi-layer second order radiative transfer model similar to the MIMICS [37] model used in Imhoff [38] and the UTACAN model used in Woodhouse and Hoekman [39]. It is described in Cookmartin *et al*. [13] where it was used for modelling crop backscatter and Balzter *et al*. [14] for forest applications. In the current study, RT2 was used to investigate the backscatter from the SERA forest for a range of scenarios. RT2 is a fully polarimetric, second-order solution to the radiative transfer equations that treats the vegetation canopy as a plane-stratified multilayer region over a rough surface. Its use in this instance is limited to a single plane with only vertical stems described by SERA existing over a rough surface. Here we consider only plant stems which are represented as finite-length cylinders and we consider like-polarised HH and VV backscatter due to its greater sensitivity to vertical structures. Although the HV polarisation is often quoted as being sensitive to forest biomass [40–42] its use for the particular scenario of vertical cylinders is reduced due to the lack of crosspolarising features present in these modelled forests. In the presence of volume scattering from foliage and branching elements of various orientations which offer greater sensitivity at higher frequencies the use of HV would be more applicable.

Microwave backscatter modelling from vegetation using radiative transfer (RT) theory is not a new concept with the first popular use of this method seen in Ulaby *et al*. [43]. RT2 models vegetation as a collection of elementary shapes uniformly distributed in one or more layers above a ground surface. The model is not a coherent discrete scattering model. This study uses the single trunk layer existing above the rough ground populated by vertical or near vertical cylinders. The model calculates extinction and phase matrices, according to the layer composition, which describe the attenuation and scattering of the energy. RT2 is of second order, incorporating direct backscatter, layer-ground interactions and layer-layer interactions. The default angle of incidence is chosen to be 35 degrees.

Airborne SAR experiments are typically carried out for incidence angles ranging from 25° to 60°, and most indicate that the preferred incidence angle is in the range 40°–45°. However system considerations for ESA's BIOMASS mission are expected to favour steeper incidence angles [44]. Currently, the minimum incidence angle is set to >23°. In a study on the sensitivity of the SAR intensity (HV) to biomass [45], similar backscatter coefficients were obtained at 23° and at 40° for biomass higher than 50·tha^{-1}, whereas for lower biomass, the backscatter signal is higher at 23° in line with current research based on airborne SAR tomography. This research suggests that observations at incidence angles of 20°–30° may increase the ground-to-volume scattering ratio, hence increasing the error in biomass retrieval based only on HV intensity. Hence the use of 35 degrees in this study as the sole incidence angle as it lies equally between the values of 25 and 45 as used in typical P-Band studies and in particular in the examination of both steep and nominal SAR configurations as investigated in Dubois-Fernandez *et al*. [45]. To model ground scattering a consistent model of a rough dielectric surface specified by an appropriate RMS height and correlation length is used throughout the study which is modelled to suit the applicability requirements for long wavelength interactions [46]. Soil moisture and roughness are maintained at constant levels. The ground susceptibility model used in RT2 is taken from an empirical model found in Hallikainen [47] which allows the proportion of sand and clay to be specified along with a volumetric moisture component. Similarly the dielectric properties of the stems are maintained at a constant value for each modelled species with plant susceptibility specified in RT2 using the dual dispersion model for branches and trunks. This model is found in Ulaby and El-Rayes [48] incorporating the parameters of gravimetric moisture and temperature; both maintained in this study as constants. Similar to the MIMICS model of Ulaby *et al*. [37] the outputs of RT2 are fully polarimetric and consist of the same scattering mechanisms including the trunk-ground/ground-trunk interaction. This scattering is determined by the size (for example radius, cross sectional area, volume), location, orientation and density of scattering components with the stems of the trees assumed to be randomly distributed. RT2 also calculates the transmission through each layer but for this study a single layer, the trunk layer, is all that is required.

Due to the limitations of RT2, in terms of the number of allowed scatterer sizes, each dataset representing the test stand was divided into 64 size classes (information for each single stem is recorded and used during the analysis and creation of equal size classes). These 64 size classes were then distributed within this layer. In effect the scatterers could be theoretically positioned anywhere within this layer but will always remain vertical. With this in mind the test stand parameterisation for RT2 represents the total volume and number density of individual size classes but the precise coordinates and their individual effects are not transferred from SERA to RT2. For this reason this backscatter investigation can only comment on trends of normalised backscatter over a large enough area that contains the 64 class sizes and not on the contribution of each individual tree unless considering a cohort of less than 64. Figure 2 shows a typical backscatter-volume plot produced using RT2 representing the forest scenario of Figure 1 devoid of canopy. Data are shown normalised for the full displayed hectare area and also for the quarter hectare area that the simulated forest occupies with similar trends exhibited by both.

Figure 2. RT2 HH backscatter representation of the forest depicted in Figure 1 emanating from a single stem from 40 years onwards. Backscatter in dB normalised to both 1 ha and 0.25 ha for comparison (since the location of stems only lies within a one quarter segment of the plot area).
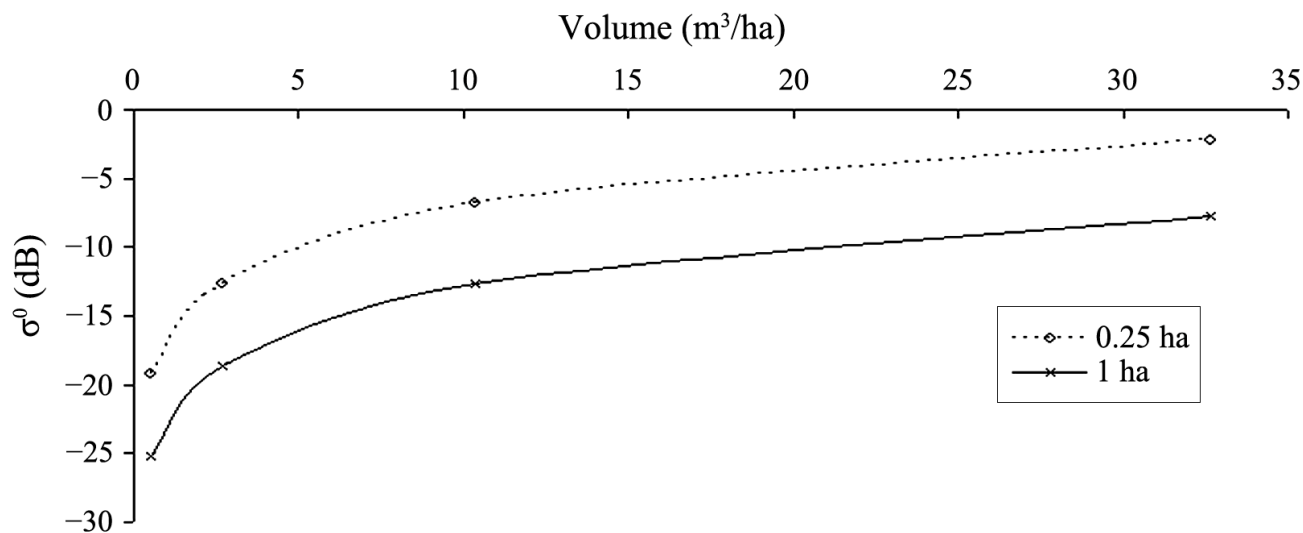
When generating forest data, SERA allows the user to determine the "world" size, starting population, and maximum number of cycles (years). In each simulation, world space was maintained as a hectare while the other values were varied in order to identify trends over a 100 year period. In this work 3 case studies are presented representing Angiosperms, Gymnosperms and a combination of both to provide a mixed species forest. These 3 "forests" are subjected to the same conditions and allowed to grow unmanaged for a 100 year duration providing a multi-age environment. Following each stage of simulated growth, separate backscatter values can be generated, and compared, for the total volume, the Rayleigh volume, and the Optical (Non-Rayleigh) volume using the limits defined by Equation (3). As well as this, theoretical values are calculated, based on Equations (1) and (2) which represent the simplistic model, to show whether the total backscatter can be represented as a saturating effect caused by transitions from one scattering regime to another in conjunction with multi age and species forest dynamics. By inferring a relationship between the Rayleigh volume and backscatter in the form of Equation (1) and between the Optical basal area and backscatter as in Equation (2), theoretical backscatter values for these components can be established and combined to provide a theoretical total backscatter from the simplistic model that is based on just two types of scattering. Comparison with the RT2 backscatter predictions is then possible. Multifrequency analysis can also be carried out to aid investigation and potentially be used in the future to infer an inverse relationship between wavelength and forest saturation age. This process will provide further evidence as to the radius-wavelength ratio influence on the total backscatter in a multi species and age environment.

For each species composition, the variations of volume, basal area, number density, and height were investigated to highlight significant links between backscatter and forest constitution and examine the feasibility of representing backscatter using the simplistic model through comparison with the RT2 model data. All of the following work is carried out using SERA to generate the forests, and the RT2 model and the simplistic theoretical model to generate comparative backscatter data sets. Data analysis in this study is largely concerned with how multi age and species forest structure influences total

backscatter particularly through variation of the forest parameters directly associated with Optical (total basal area) and Rayleigh (total volume) scattering.

3.1. Modelling Scenarios

Three scenarios were examined; these scenarios were the forest configurations of (a) *Abies alba* (Gymnosperm); (b) Generic Angiosperm (Angiosperm); and (c) Mixed Species (Gymnosperm and Angiosperm). Figure 3 shows a typical visualisation of SERA derived data at 0, 25, 50, 75 and 100 years. The forest shown is the *Abies alba* forest, (a). Each forest can be viewed in a similar fashion using horizontal and bottom up views.

Figure 3. Horizontal and bottom-up representation of *Abies alba* forest before canopy removal. Snapshots at (**a**) 0, (**b**) 25, (**c**) 50, (**d**) 75 and (**e**) 100 years. Plots are 100 m^2. Brown represents stems, darkness of green represents level of canopy shading, for example bright green represents unshaded canopy. Blue represents sky, indicating zero canopy cover.
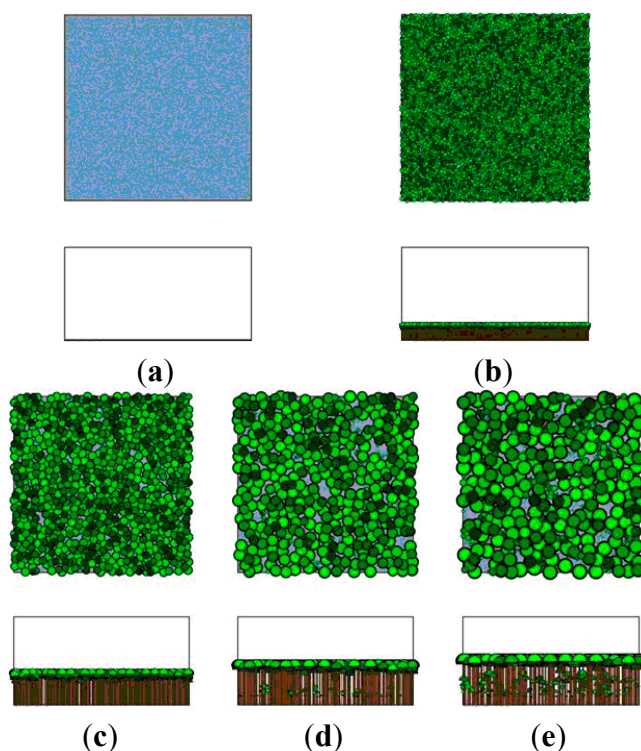

Each modelled forest examined in this study is based on an initial planting density of 25,000 trees, to mimic the planting conditions of the empirically monitored forest of *Abies alba* referred and compared to in the initial SERA publication [12]. The numerical description of the forest dynamic over time is given in Table 1 for scenario (a). The data from this table representing backscatter against volume per ha are plotted in Figure 4. Figure 5 shows how the number of trees and total basal area in each forest composition vary over time.

The backscatter for *Abies alba* follows the typical saturation pattern commonly reported in forest SAR studies [49,50]. As the forest volume increases, the returned backscatter does so also. When the volume reaches a certain limit the increase in backscatter per unit volume reduces significantly until under certain circumstances the increase saturates, signalling a zero increase in backscatter per unit

volume. This is seen at approximately 650 m³/ha, a significantly large volume density but the steady decline in backscatter change with volume begins at a much lower value. In a similar fashion Baker *et al.* [49] noted that the "gentler rise" occurred at ages beyond 20 years for empirically monitored Corsican Pine, similar to what is seen here for the modelled *Abies alba*. The most common explanation for this saturation behaviour is given as the attenuation resulting from the increasing density of canopy components. This would appear to be an acceptable explanation when taking into account the visualisations shown in Figure 4 but for the scenarios modelled here all backscatter is generated for a single stem layer with a zero canopy component, reducing the likelihood of such a cause. Alternate explanations may be considered for this scenario bearing in mind the backscatter contributions of Rayleigh and Optical scatterers when plotted against volume, with modelled Rayleigh scattering at high volumes appearing to contribute very little to total backscatter. The contribution of these different scattering regimes will be a warranted approach if the simplistic model incorporating these scattering variations produces backscatter data similar to that modelled using RT2. While we can show that saturation can exist in the single stem layer scenario, the single scattering layer will not saturate due to opacity. It is then important to note at this early stage that this study does not investigate the level to which saturation is caused by one or the other effects referred to above but only examines possibilities in the absence of attenuation and how these considerations using the simplistic model impact the comparison with RT2 predicted data.

Figure 4. RT2 P-Band HH Backscatter and volume values shown with respect to the visual appearance of the *Abies alba* forest at 0, 25, 50, 75 and 100 years old, left to right respectively. Note that backscatter and volume values are only representative of the stems.
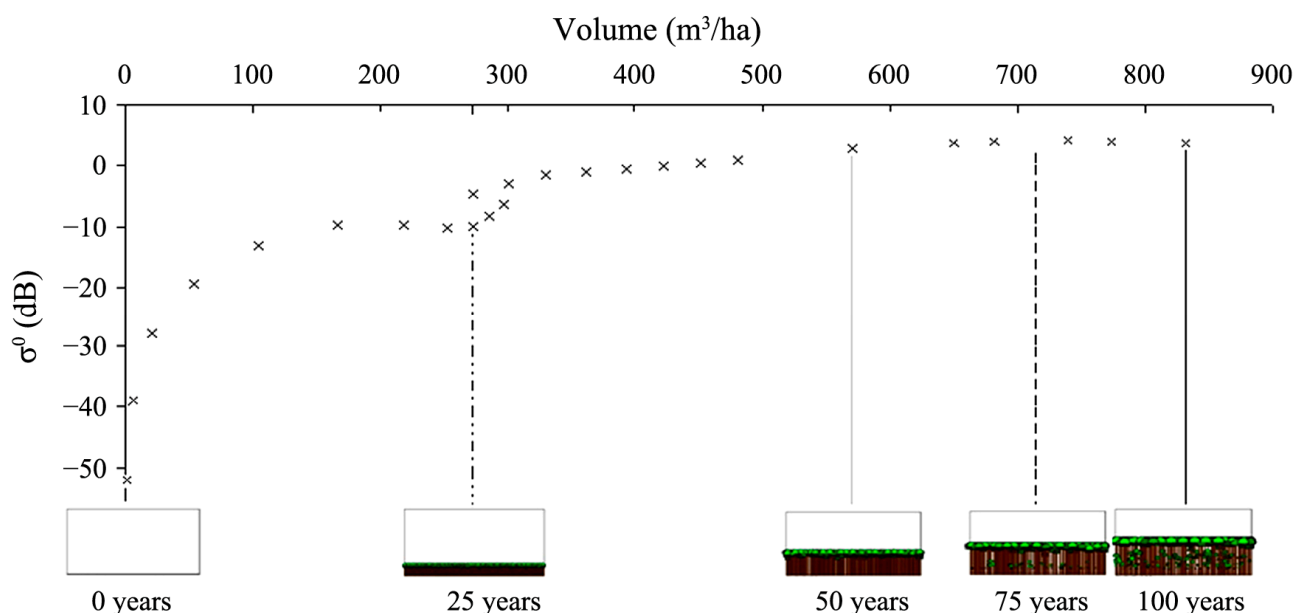
As the volume values and visualisations suggest, there will inevitably be an increase in attenuation as a forest's size increases. At very short wavelengths the smaller canopy branches will cause the attenuating effects but at longer wavelengths the attenuating effects of the canopy will have less influence. With the removal of canopy considerations the backscatter values are therefore not influenced by canopy attenuation. Tables 1 and 2 provide information regarding stem volume per hectare, basal area per hectare, H100 (mean height of the 100 trees with the largest diameters at breast

height within a hectare), volume of stems scattering optically within a single hectare, and volume of stems Rayleigh scattering within a single hectare according to the limitations of Equations (3) and (4) and the assumptions made regarding Mie scattering. The inconsistency evident in the backscatter curve of Figure 4 can be explained through numerical evaluation of Table 1 which indicates backscatter levels are susceptible to the signal disruption/attenuation from the vast numbers occupying the limited available space. This in turn produces large and subsequently unsustainable levels of basal area values (comparison with Table 2 affirms this). If the forest consisted of a large proportion of Rayleigh scatterers at this volume the discrepancy could also result from the dominance of size influence over number density [10] with two equal volume plots producing different backscatter values as a result of one plot comprising fewer but larger trees.

Figure 5. Stem number thinning with passing years for the three cases. Circle area is in proportion to plot basal area with relative changes in size representing relative basal area changes. Centre of circle indicates data point location.
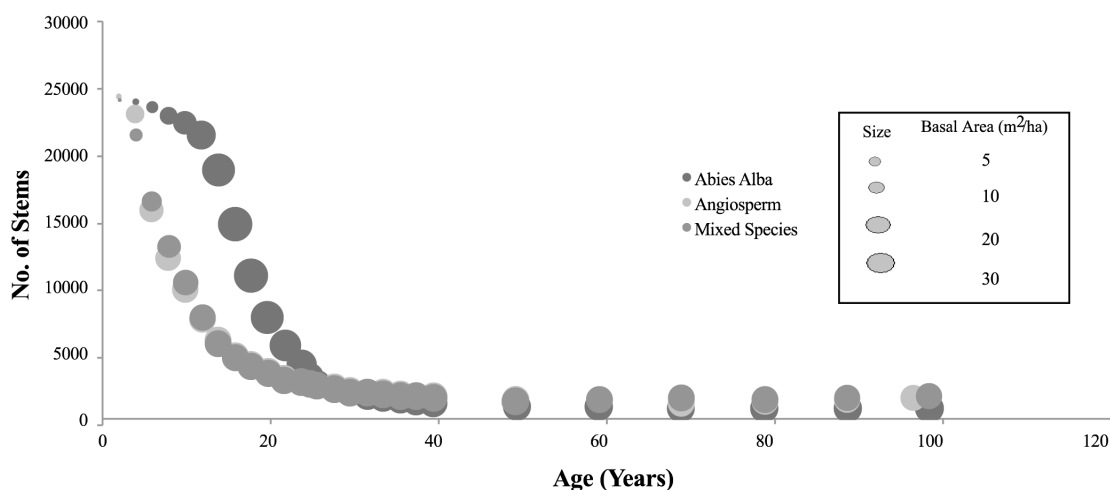
In Brolly and Woodhouse [8] it was predicted that saturation effects are due to the increasing presence of optically scattering branches or stems; a situation only possible at longer microwave wavelengths. In that work the forest was controlled by the presence of mono-sized stems so that the transition from Rayleigh to Optical scattering could be easily monitored. In this work using SERA the more realistic scenario of multi sized, multi-generational, and also multi species stems occupying any particular stand are considered.

The contribution to the total backscatter of the different sized stems is expected to show that complete saturation (meaning constant backscatter with increasing volume) is very rarely achieved in nature due to the continual regrowth taking place beneath the dominating upper canopy, especially upon senescence. A more common occurrence is then for a gradual change in backscatter per unit volume to be observed with possibilities for both positive and negative correlation. This is an expected consequence due to the changing number density of Optical scatterers resulting from thinning and growth of existing trees. Such behaviour suggests that a climax forest can continue to have a volume contribution from Rayleigh scatterers in both the canopy and from the floor, dependent on incident wavelength. Comparison between the RT2 modelled backscatter and that produced using the simplistic model will also provide evidence for the applicability of the work of Brolly and Woodhouse [8,10] for

application to more species and temporally heterogeneous environments than the simple mono culture scenarios previously examined.

Table 1. *Abies alba* forest data modelled using Spatially Explicit Reiterative Algorithm (SERA), presented over a growing period of 100 years.

Age (Years)	Stems	Vol. (m³/ha)	Basal (m²/ha)	H100 (m)	Opt. Vol (m³/ha)	Ray. Vol (m³/ha)
0	24,809	0.00	0.00	0.02	0.00	0.000
2	24,409	0.06	0.26	0.23	0.00	0.059
4	24,010	1.08	1.68	0.65	0.00	1.084
6	23,562	6.41	5.27	1.22	0.00	6.406
8	22,950	21.79	11.57	1.89	21.72	0.077
10	22,318	53.76	20.57	2.65	53.76	0.000
12	21,403	105.29	31.29	3.46	105.29	0.000
14	18,829	166.42	40.19	4.33	166.42	0.000
16	14,720	218.18	43.92	5.24	218.18	0.000
18	10,753	253.18	43.32	6.19	253.18	0.000
20	7598	272.58	40.26	7.17	272.58	0.000
22	5477	286.08	37.04	8.18	286.08	0.000
24	4048	296.66	34.11	9.22	296.66	0.000
25	3128	271.53	29.81	9.67	271.53	0.000
26	2685	272.81	28.35	10.14	272.81	0.000
28	2227	300.30	27.82	11.57	300.30	0.000
30	1926	330.27	27.71	12.78	330.27	0.000
32	1716	361.67	27.95	13.87	361.67	0.000
34	1558	392.70	28.27	14.86	392.70	0.001
36	1429	422.11	28.61	15.76	422.11	0.003
38	1317	450.68	28.98	16.60	450.68	0.003
40	1245	480.89	29.56	17.38	480.89	0.005
50	896	570.17	29.33	20.57	570.16	0.012
60	872	649.25	29.84	22.92	649.23	0.022
70	838	681.19	28.95	24.84	681.17	0.023
80	854	739.32	29.71	26.46	739.30	0.021
90	839	774.21	29.83	27.80	774.18	0.027
100	818	831.55	30.85	28.98	831.53	0.022

Although the general saturation curve with increasing volume is manifest in each dataset, the effect of a rapidly increasing basal area and the subsequent drop off to a more sustainable level appears to have a profound effect on backscatter. In a similar way to that seen in Baker *et al*. [49], it would appear that single species gymnosperm forests have a tendency to overstretch their resources in terms of basal area accumulation per area. In Figure 4 this area of change is shown to coincide with the fluctuation in backscatter around 270 m³/ha shown for the RT2 modelled backscatter data. This occurrence highlights how "self-thinning" and basal area may directly influence backscatter levels.

The backscatter data for forest scenarios (b) and (c), are shown in Figure 6 for RT2 simulated total backscatter, Optical backscatter and Rayleigh backscatter with each forest exerting very similar behaviour. The mixed species forest composition emphasises the competitive dominance of

angiosperms over gymnosperms as time elapses, with the forests of the generic angiosperm and mixed composition almost identical in both number (Figure 5) and structure as the forest matures. As a result the backscatter data is very similar. Table 2 shows the specific data for the generic gymnosperm forest.

Table 2. Angiosperm forest data, modelled using SERA, presented over a growing period of 100 years.

Age (Years)	Stems	Vol. (m³/ha)	Basal (m²/ha)	H100 (m)	Opt. Vol. (m³/ha)	Ray. Vol. (m³/ha)
0	24,825	0.00	0.00	0.04	0.00	0.000
2	24,400	0.97	1.21	0.80	0.00	0.971
4	23,039	44.12	12.68	3.77	43.95	0.445
6	15,733	153.33	21.68	7.51	153.33	0.000
8	12,167	227.12	24.49	9.76	227.12	0.003
10	9776	277.03	25.63	11.36	276.87	0.167
12	7471	316.11	26.39	12.60	315.91	0.201
14	5871	348.82	26.89	13.62	348.70	0.116
16	4776	377.12	27.29	14.47	377.01	0.117
18	4043	397.31	27.31	15.20	397.24	0.073
20	3519	418.74	27.55	15.85	418.66	0.084
22	3087	437.81	27.78	16.43	437.73	0.080
24	2814	457.96	28.16	16.95	457.91	0.053
25	2664	464.69	28.16	17.19	464.63	0.063
26	2527	471.38	28.17	17.43	471.31	0.063
28	2364	488.82	28.50	17.86	488.76	0.068
30	2141	496.76	28.28	18.26	496.69	0.074
32	2038	507.91	28.36	18.64	507.85	0.067
34	1954	515.26	28.26	18.99	515.20	0.057
36	1869	521.50	28.14	19.32	521.44	0.060
38	1763	531.02	28.20	19.63	530.96	0.060
40	1683	537.98	28.17	19.92	537.92	0.063
50	1415	539.36	27.61	21.17	559.31	0.052
60	1407	568.25	26.98	22.19	568.20	0.048
70	1232	586.58	27.08	23.03	586.55	0.035
80	1262	587.96	26.50	26.51	587.90	0.056
90	1415	577.94	25.63	24.35	577.88	0.052
100	1556	556.05	24.68	24.74	555.99	0.060

In both cases the total backscatter appears to progress in a more uniform way than for the *Abies alba* scenario of Figure 4. Thinning is at a much greater level and basal area and volume increase at a steady rate with no obvious overexpansion. The mixed species forest example consists of 6 variations of species. These six comprise *Abies alba*, generic angiosperm with additional shade constant, generic angiosperm, generic gymnosperm, generic gymnosperm featuring the *Abies alba* specific photosynthesis constant, and generic gymnosperm with the *Cryptomeria* photosynthesis constant. When planted in equal numbers the dominant species after 100 years becomes the generic angiosperm with a gradual reduction in the overall percentage of gymnosperm contribution seen from an early age.

4. Results

4.1. Forest Data Comparison of Mono and Multi Species Plots

In order to apply the theoretical values of backscatter based on Equations (1) and (2), the backscatter must be separated into both Rayleigh and Optical scatterers according to Equation (3), with Optical denoted as anything non Rayleigh. With the stems separated into their respective scattering size classes the backscatter created by the Rayleigh scatterers can be plotted against the squared volume that they occupy. Similarly the Optical backscatter can be plotted against the total basal area. By doing this, the constants associated with Equations (1) and (2) can be obtained and used to predict the theoretical backscatter values for the entire volume based on the combined results of the simple equations within the simplistic backscatter model. The results of this process indicate whether the backscatter and saturation within a forest can be considered a simple combination of two scattering types through comparison with the trends exhibited by the RT2 modelled backscatter data.

The data provided by this process has already been shown to produce negligible Rayleigh contribution at high volumes but a noteworthy one at low volumes (Figure 6). In the presence of a canopy (not modelled here) there would be a significant increase in Rayleigh scatterers at all stand ages with the contribution to the total backscatter expected to be most influential on the backscatter trends at low forest volumes. At higher forest volumes the size of the largest Optical scatterers will be much larger proportionally to the Rayleigh scatterers, in such a case the Rayleigh contribution gradually becomes less significant even with the increase in Rayleigh numbers brought about through canopy consideration. In Brolly and Woodhouse [10] it was shown that the contribution of Rayleigh backscatter is most dependent on scatterer size while optical scatterers are more dependent on number of scatterers. As a result, the peak backscatter response will be located at the transition between these two regimes for most realistic crown architectures. The peak backscatter response is not always associated with the stem layer, particularly at higher frequencies. In light of this there exists the possibility that the inclusion of crown scattering components will increase the number of scatterers within the size range of the Rayleigh to Optical transition. This will be of most significance when the secondary or even tertiary branches of the largest trees are considered Optical scatterers or within close size proximity to this transition region. This will increase the total backscatter value.

By combining the simple theoretical Rayleigh and Non-Rayleigh backscatter datasets, generated using the simplistic model, the robustness of the relationship is tested through its correlation with the total backscatter produced using the RT2 modelled backscatter. High correlation would suggest a consistency between the simple model and the full radiative transfer model. In turn, this would support the assertion that forest backscatter behaviour is significantly influenced by the ratio of stem size to wavelength [38]. Additionally, this could provide further explanation for the saturation effect in a multi-faceted forest as forest volume increases beyond certain limits. In the manner of the Matchstick model [8] and SERA this is brought about by a reducing number of stems (Figure 5) individually increasing their volume and basal area (Figure 7). The influence of "self-thinning" on backscatter is highlighted through these relationships. Importantly, reductions in stem number are also shown to reduce the effect of signal interference so that any saturation can be a result of the physical laws of scattering and not necessarily attenuation.

Figure 6. RT2 modelled P-Band HH backscatter associated with SERA generated stem forests over a 100 year period. RT2 backscatter generated for the Total forest, Optical forest and Rayleigh forest according to limits of Equation (3) for forest scenarios (b) and (c). Break in line continuity represents volumes at which type of scattering is not present.
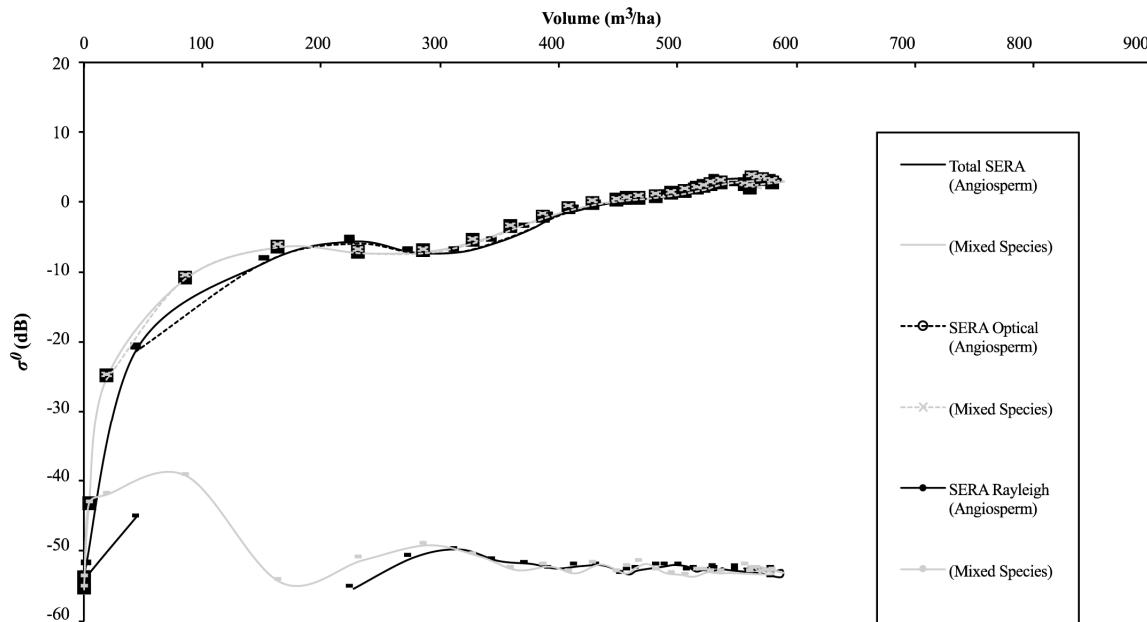
Figure 7. Volume per hectare of stems plotted against Basal Area per hectare for three cases. Circle area represents relative number of stems, the larger the area the larger the number of stems. Centre of circle indicates data point location. Initial planting density 25,000.
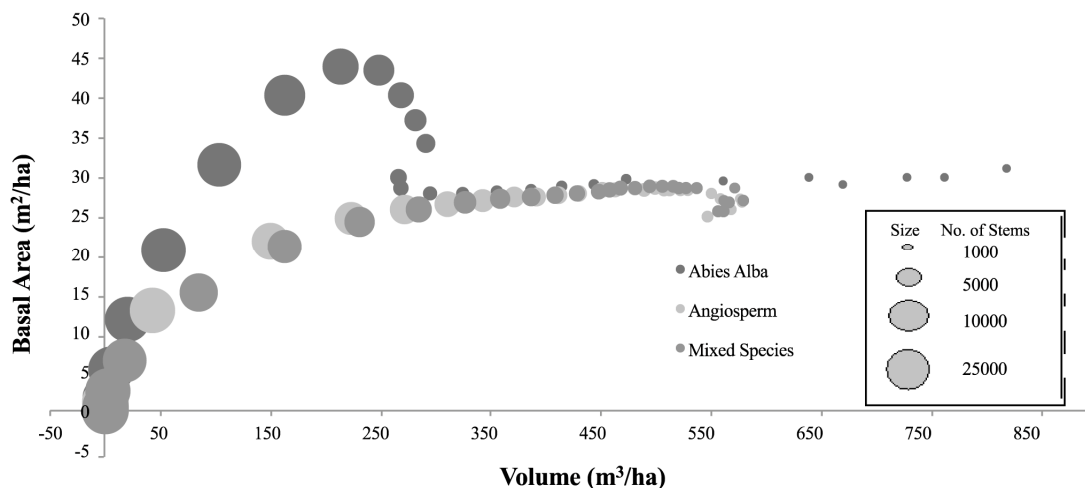
The thinning component of Woodhouse [3] considered that at a particular volume the forest can adopt a thinning exponent indicating a constant forest basal area. Such a thinning routine would be implemented in a climax forest when finite resources are fully utilised. At different stages of a real forest's growth this thinning value is likely to vary. These variations are often noted as an increasing rate of thinning with age as volume increases beyond forest maturity. If the vast majority of significant scatterers are larger Optical scatterers (a feature more common in a mature forest when using long microwaves) and the basal area remains approximately constant, then saturation of backscatter will be as predicted by Equation (2). Such a theory suggests that the reason the values of volume at saturation

points can vary for the same incident wavelength is that it is the distribution of stem sizes for any particular volume that determines the saturation limit, not the volume directly. If resources are limited the saturation would be expected to occur at a lower volume as lower basal areas will be present with fewer trees able to grow to the required Optical scattering diameters. Consequently the forest volume will be low. Conversely, if there is an abundance of trees with the same diameter then saturation would be expected at a higher volume and basal area. In a similar fashion, saturation could be described by age variations and through association with the types of age stand structures that exist (TASS) [51].

The similarities and differences in the backscatter of the three data sets (scenarios (a), (b), and (c)) can be related to both Figures 5 and 7 showing how basal area and volume fluctuate but also how the stem numbers thin with age. The differences between *Abies alba* and the other cases are obvious, particularly over the first 30 years of growth (up to 300 m^3/ha) when the recorded basal areas reach unsustainable levels before a reduction to values comparable to Angiosperms. With regard to the importance of volume and basal area in determining saturation, SERA predicts that forests (through the trees within them) consistently grow to reach an optimum condition. This relationship between the optimum basal area and volume of particular species can be seen in Figure 7. As the dominant species in the mixed forest is the Angiosperm it is no surprise that the cases of Angiosperm and Mixed species data converge at higher levels of basal area and volume. The *Abies alba* data on the other hand shows the behaviour seen in mono species gymnosperm plantations of over extension in terms of basal area and then rapid die back [49] suggesting less nutrient requirements per tree at younger ages. Correlation between volume and basal area is still evident between the different species in Figure 7 but only at volumes below 100 m^3/ha and then again above 300 m^3/ha. Overall, from the forest data produced by SERA, a particular stand area has the ability to sustain a much larger volume of *Abies alba* than the Angiosperm species, with the Angiosperms appearing to reach their optimum/maximum volume at approximately 550 m^3/ha while *Abies alba* for the same area does not reach its optimum within the 100 year study limit. As for basal area, for each case the optimum basal area is in the region between 25 m^2/ha and 30 m^2/ha with a reduction in basal area only occurring if the optimum/maximum volume has been reached or basal area over extension occurs. In scenarios such as this the constraint in volume appears to dominate over basal area. With height continuing to increase, the forest must therefore scale back in number density to avoid exceeding this optimum volume value.

*4.2. Backscatter Consequences of Scattering Regime Transitions*

Backscatter is shown to increase with volume using both the simplistic model and the RT2 model. This is irrespective of the large variations in basal area seen for the *Abies alba* case visualised in Figure 7. With respect to volume the backscatter in general appears slightly higher for scenarios (b) and (c) using both backscatter models, although only conclusively at levels above 300 m^3/ha corresponding to the significant basal area variation. As for the thinning, the rate for *Abies alba* is much more variable in comparison to the other two cases as is apparent through the circle area representation of number density shown earlier in Figure 5.

With regard to the findings concerning basal area and volume constraints, the SERA-RT2 backscatter, and the SERA-simplistic model backscatter, both corresponding to the total volume per ha, are plotted in Figures 8–11 for the 3 examined forest scenarios. The backscatter appears to follow the expected trajectories—a growing forest initially, then as it matures it thins close to a level that

maintains basal area [3] and as a result approximately constant backscatter is recorded as volume increases to allow larger stems into the Optical scattering regime. In each case the theoretical trajectory matches well with the P-Band RT2 generated backscatter above volumes of 300 m^3/ha. At these volumes the majority of stems are scattering Optically and with forest basal area values consistently within the region of 25 m^2/ha to 30 m^2/ha the backscatter assumes a very small fluctuating rate of change. This backscatter increase corresponds with the level of basal area increase up to volumes of approximately 600 m^3/ha in the cases involving angiosperms and to the end of the data range for the *Abies alba* case. If the 600 m^3/ha level is assumed to be the optimum (or maximum) volume sustainable by generic gymnosperms then up to this volume level the relationships laid out in Equations (1) and (2) hold. Beyond this level SERA predicts that the focus behaviour of the forest is altered in an attempt to balance volume and basal area constraints rather than the previous priority of increasing volume while maintaining basal area. The basal area increases are represented by the increases in circular area representing data points in the figures in question. It is apparent that basal area varies very little above 300 m^3/ha but increases gradually prior to this. This is true with *Abies alba* in spite of its rapidly increasing and subsequently decreasing basal area value.

Significantly in the case of *Abies alba* the theoretical interpretation of backscatter data using the simplistic model does not fit the RT2 data estimations at volumes between 50 and 300 m^3/ha, Figure 8. In this region of volume, the basal area reaches unsustainable levels as shown in Figure 7. As a result it would be expected that the backscatter will be much higher in this region due to its dependence on Optical backscatter. This is manifest in Figure 8 through the theoretical simplistic model representation but it is clear that the RT2 model data does not follow the theory offered by the simplistic model in this region, with the backscatter being comparatively underestimated. Applying the theory to the work of Baker *et al*. [49] on Corsican Pines would result in a similar outcome, with no great increase in backscatter seen for the large basal area increases exhibited by the forest. Reasons for this anomaly could be assigned to the overcrowding of the forest impacting on the backscatter returns both using the RT2 model and in the empirical environment. The nature of the forest at this moment in time is such that, according to the classification used here, there are no Rayleigh scatterers within the forest. As the volume increases from 50 m^3/ha to 300 m^3/ha there is no further Rayleigh contribution under the constraints of Equation (3). The same dataset, with VHF backscatter, does not suffer from the same extent of overestimation made by the simplistic model. The volumes at which the basal areas are elevated in the VHF case lie within the Rayleigh region and therefore the backscatter is correlated with the volume squared of the target coupled with the longer, less attenuated wavelength of VHF, Figure 9. For *Abies alba*, at both P-Band and VHF, there is a mismatch at the transition from Rayleigh to Optical scattering between the theory and the backscatter, the anomalous results showing a data spike in the theoretical backscatter. Since the boundaries of Equations (3) and (4) are not exact and liable to vary on a small scale, anomalous results would be minimised by considering such variations closely. Under thinning conditions associated with Angiosperms, the impacts at these transition zones are greatly reduced. This may be due to the wide variability of stem radii in Angiosperm communities which allow a more even spread of values while for gymnosperms there is less variation and larger radii steps due to annual accumulation rates.

Figure 8. P-Band HH *Abies alba* backscatter with respect to volume per hectare. SERA-RT2 generated backscatter in conjunction with SERA-theoretical calculation of backscatter with respect to volume. Circle area signifies relative basal area quantity per hectare with centre of circle indicating data point location.
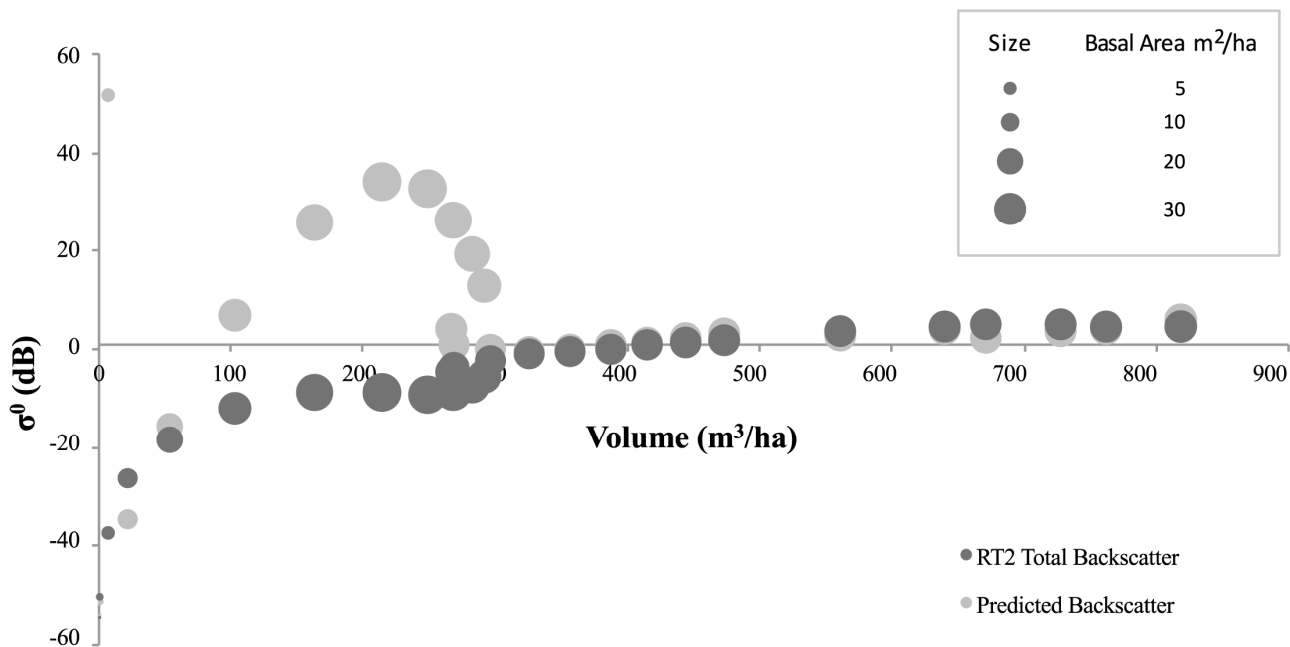

Figure 9. VHF HH *Abies alba* backscatter with respect to volume. SERA-RT2 generated backscatter in conjunction with SERA-theoretical calculation of backscatter. Circle area signifies relative basal area quantity per hectare with centre of circle indicating data point location.
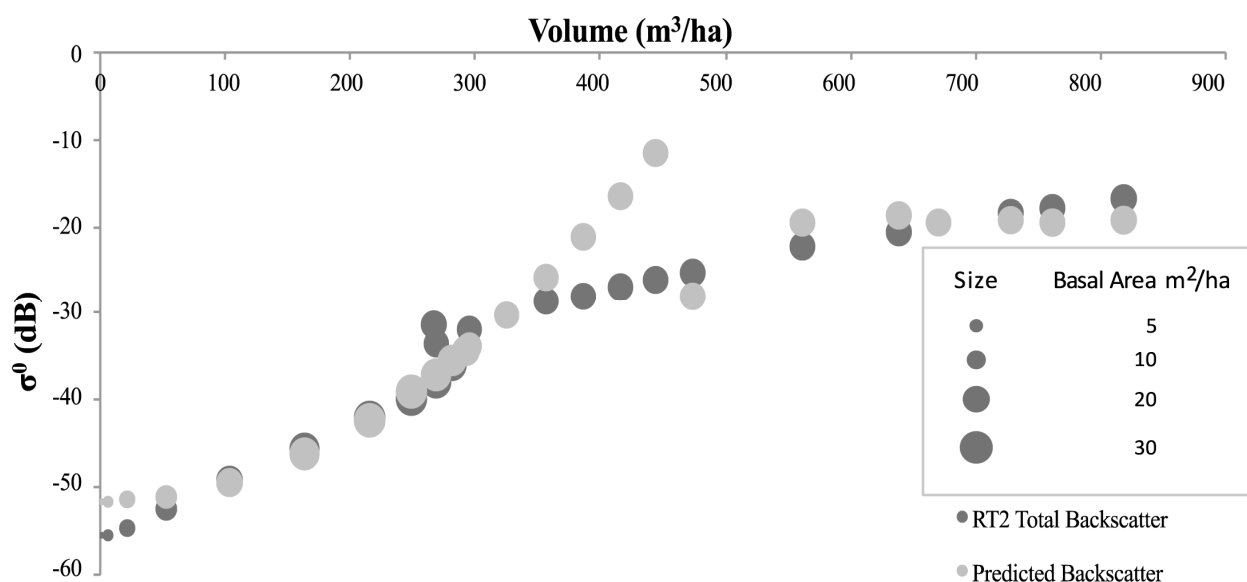
For the cases involving Angiosperms there is a distinct correlation between the theoretical backscatter generated by both the simplistic model and the RT2 model. The anomalies identified within the *Abies alba* datasets are not observed here and the two theoretical backscatter datasets correlate extremely well. The success of interpreting forest scattering using the "Matchstick Model"

theory [8], for a spatially and temporally varying forest, in conjunction with the trends of the RT2 model are evident through the observed correlations. The R^2 values for P-Band and VHF correlations between the theoretical datasets are shown in Table 3. The effect that the overextended basal area has on the *Abies alba* data is only seen at P-Band, as the VHF data is more dependent on the square of the volume in the region of over-extension. The spike in the simplistic model backscatter is also much more significant at P-Band.

Figure 10. P-Band HH Generic Angiosperm backscatter with respect to volume. SERA-RT2 generated backscatter in conjunction with SERA-theoretical calculation of backscatter with respect to volume. Circle area signifies relative basal area quantity per hectare with centre of circle indicating data point location.
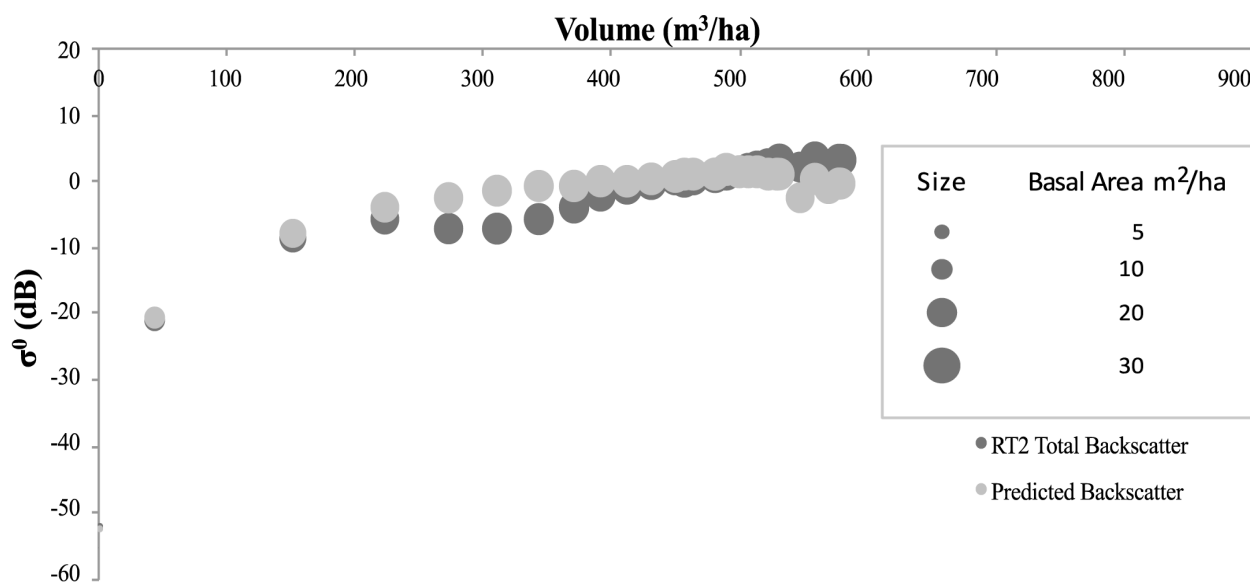
In order to understand the low correlation between RT2 and the simplistic model theory, exhibited through the *Abies alba* backscatter data, the thinning rate of the *Abies alba* stand was manually altered, as a test, to that of the levels of the Angiosperm and Mixed species forests (through the removal of the smallest stems). This allowed the scattering regime theory used in the simplistic model to better match the trends generated in the RT2 backscatter that correspond to the new thinning regime (new R^2 value of 0.95). Complications related to basal area over-expansion were then removed from the scenario. This crude matching of thinning, which leaves the largest stems intact, and the resultant high correlation are achieved with very little volume variation from the original data and highlight how attenuation of this type is only a problem in high density areas where individual basal area is also high, as is seen in Figure 8. In essence the backscatter produced by the RT2 model, and evidently empirical studies, in these instances appears limited by the density of scatterers and individual high basal areas but not necessarily the total volume. Specular scattering from the surface may then contribute more, as well as there being a reduction in backscatter as a consequence of stem-ground scattering mechanism attenuation due to the combination of close proximity and high stem basal areas (see Figure 3 at 25 years as an example). Critically, data from this study has not relied on canopy attenuation as the source of saturation behaviour. The reduction in number density with increasing age and volume (Figure 5) and the reduction in basal area following the over expansion (Figure 7) reinforces this

understanding as the backscatter returns to theoretical levels once thinning has resolved the number density issue, all while volume continues to increase. Attenuation resulting from interactions with stem components in high number density forests requires a more in-depth study than is offered here.

Figure 11. P-Band HH Mixed species backscatter with respect to volume. SERA generated backscatter in conjunction with SERA-theoretical calculation of backscatter with respect to volume. Circle area signifies relative basal area quantity per hectare with centre of circle indicating data point location.
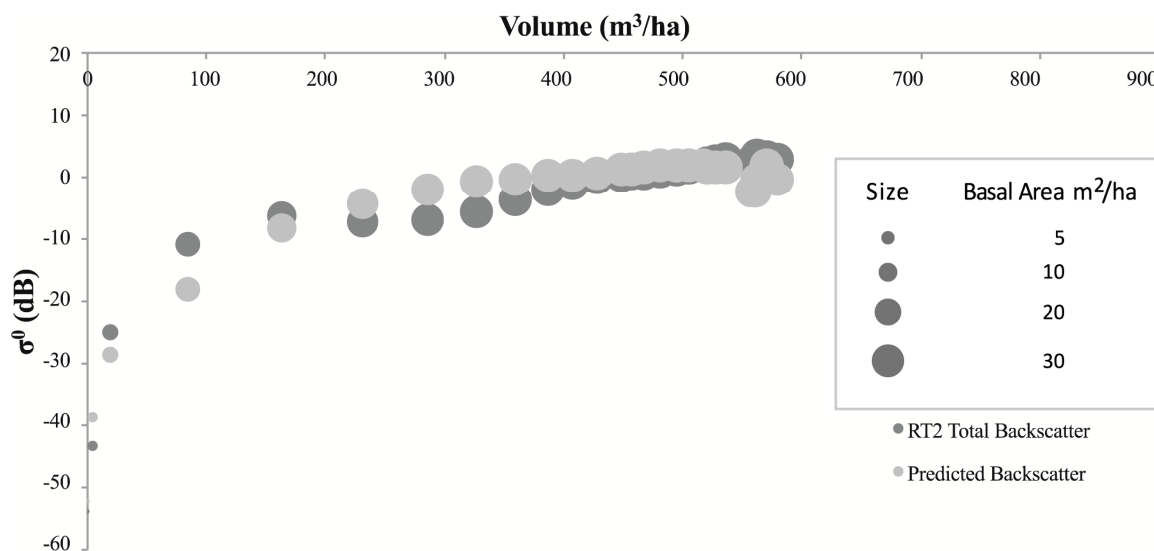

Table 3. Correlation between theoretical values (based on relationship with basal area) and RT2 backscatter over a 100 year period starting from an initial planting density at year 0 of 25,000 stems.

Species	R^2	
	P-Band	**VHF**
Abies alba	0.45	0.92
Angiosperm	0.96	0.90
Mixed	0.97	0.92

Multifrequency backscatter analysis of the mixed species forest of scenario (c) from Section 3 is visualised in Figure 12. The expected trend in backscatter behaviour is exhibited with saturation occurring at higher volumes for lower incident frequencies with the highest frequencies, as expected, producing the highest intensity of backscatter. Of particular interest is the fact that this typical behaviour is exhibited in the absence of canopy attenuation with saturation exhibited within the volume range of 0 to 500 m³/ha for frequencies from 5 GHz (C-Band) down to 429 MHz (P-Band). Low saturation volumes apparent here can be explained by the consistency in basal area following transition to Optical scattering which occurs at lower volumes for higher frequencies due to increasing sensitivity to smaller scatterers. The 50 MHz data (VHF) on the other hand does not show saturation behaviour within the displayed volume range. This is in accordance with the simplistic model theory that suggests a transition of dominant Rayleigh scattering to Optical scattering at much higher volumes than for the other frequencies shown.

Figure 12. Multifrequency RT2 model HH backscatter for mixed forest of scenario (c) (Section 10.5) against volume per hectare. Note that these trends are a result of vertical stems present in a single layer in the absence of canopy scattering, and therefore not influenced by attenuation. 25,000 initial stems for each case.
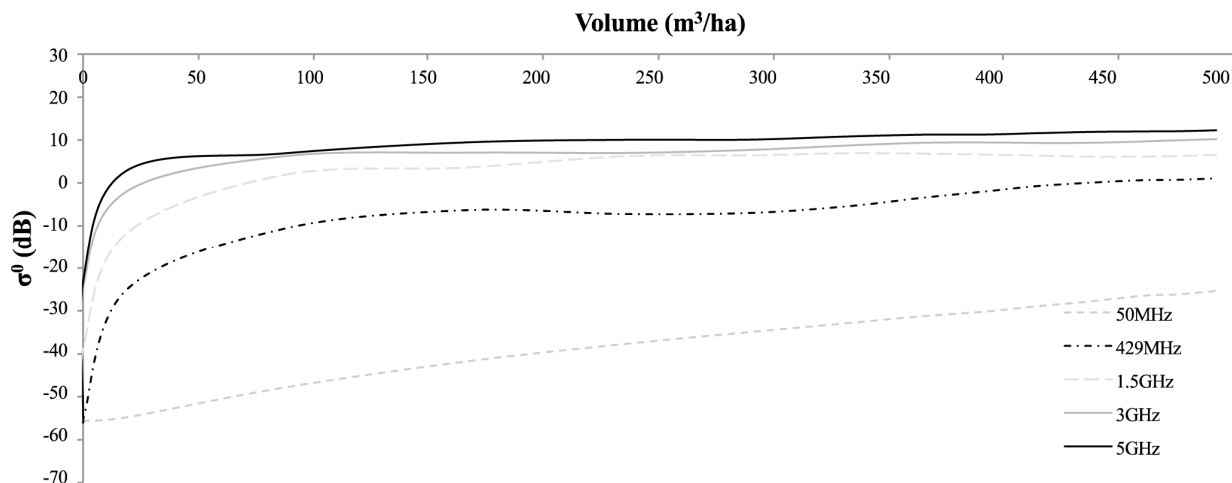
5. Discussion

A forest growth model (SERA) was used to investigate the theoretical possibility of forest SAR backscatter saturation being caused by the inherent physics of electromagnetic scattering in relation to forest dynamics rather than due to commonly held assumptions of increased opacity of the canopy. The assumption is such that as the height of a forest increases, the ability of an EM signal to penetrate through the forest canopy towards the ground is reduced. The existence of attenuation in relation to EM waves is not debated here but rather we consider its importance to the particular scenario of long wavelength SAR backscatter saturation by modelling backscatter trends with a single layer of stems. Such a "Matchstick model" approach [8] uses solely the wavelengths most sensitive to the larger forest components, *i.e.*, the stems, which can contain up to 90% of a forest's biomass [31]. As a result of this, the attenuating effects of the canopy are removed physically and theoretically from the scenario, allowing an investigation of the relationship between wavelength, stem size, and stem number density. It has been reported elsewhere that radar backscatter can saturate over a variety of different forest volumes, dependent upon the wavelength but also the forest type [52]. Unlike the "Matchstick model" approach, here the modelled forest supports multi-aged stands in mono and mixed species stands. The ability of the simplistic model to predict backscatter behaviour in comparison to that produced using the RT2 model is examined with consideration paid to the environment and dynamics of the modelled target forests.

In this study the frequency 429 MHz (P-band) is the principal frequency of investigation with a wavelength of 0.7m. Many studies have quoted this frequency to saturate at between 100 to 200 t/ha (approximately 167 m^3/ha–333 m^3/ha) [44], but as the theories presented in this study would suggest, these saturation figures are not dependent solely on the biomass of the forest, but also on the size of its constituent components and the methods that control size dynamics (*i.e.*, human, or natural thinning). In a typical forest 333 m^3/ha represents a biomass at which the forest has had several years of growth and has become mature and climactic. When a forest has achieved this status the most consistent forest

parameter is the total basal area over time of the stand. Using SERA [12] and simulating, from conception, 3 separate forest environments consisting of *Abies alba* (*a*), generic gymnosperm (b) and a forest consisting of mixed species (c), each forest has shown that for this volume the change in basal area per year of growth is less than 1% every year. With the nature of Optical scattering being proportional to the basal area increase of the stand, when stem length is proportional to diameter [32,35], the backscatter would be expected to saturate if the rate of increase of basal area with volume stagnates in a purely Optically scattering environment. According to Equation (2) the theory suggests that if there is no increase in basal area then there will be no increase in backscatter. This statement is indeed true in the idealistic scenario of the forest being entirely devoid of Rayleigh scatterers, but with the existence of regrowth in each of the simulated forests there remains a small contribution from Rayleigh scattering proportional to its volume squared [6] (Equation (1)). Additionally in the natural world the presence of dead wood and Rayleigh scatterers in the canopy, both not considered here by SERA, will contribute to the total backscatter, thus causing further deviation from the theory. Due to the nature of Rayleigh backscatter, small increases in volume will result in a much greater increase in backscatter than that caused by similar basal area increases although their net contribution will be smaller also [10]. Hence it remains a possibility that modelling forests devoid of canopy may produce what appears as complete saturation. The more likely scenario is that the dynamism of a forest in the modelled and more significantly in the natural setting will prevent complete saturation.

Figure 12 helps to explain the relationship between forest backscatter, volume, and frequency. In a single layer defined by the height of the largest stem, the trends are considered driven by stem size rather than extinction. Stable saturation is more apparent for higher frequencies as more of the forest scatters Optically. An additional complication within the modelling scenario relates to the emergence of secondary branches within the natural setting that are not modelled in this study. It is believed that these secondary branches, when of sufficient size (corresponding with increasing age of the forest), will contribute to the radar backscatter in a similar manner to that expected of young trees or saplings. Due to the nonverticality of these branches this will be most significant in the HV polarisation with less impact on the HH data where the trunk to ground double bounce dominates. The contribution of these secondary branches will therefore be minimised through both the choice of polarisation and as a consequence of the low number and therefore total biomass of these scatterers. Even at high volume densities, with thinning reducing a population of stems of 25,000 at 0 years to significantly less than 5000 by 50 years (Figure 5). Figure 6 shows how stems of the size order of secondary branches (indicated by low volume levels) can contribute significantly to total backscatter when they begin to scatter Optically but the number of stems required in this example, close to 20,000 vertical stems, is sufficiently higher than would be expected of secondary branches within a population of ~2000 multi-aged stems after 50–100 years of forest growth.

SERA has predicted that a forest will tend towards an optimum basal area with a maximum volume. In biological terms the forest can only be sustained within the confines of the allocated area and in accordance with the resources available (light, water, nutrients). When these are expended only senescence followed subsequently by regrowth or additional growth in the survivors will take place. At such times the volume and basal area will be temporarily reduced until the gap can be filled. At this point it would appear that different backscatter values to those expected are possible in response to the

change in number density and total size and structure changes of the forest. These backscatter changes are proposed to be directly related to the variation in the mix of Rayleigh to Optical scatterers resulting from mature death and regrowth.

By coupling SERA with RT2 and the simplistic backscatter model it has been shown that the Optical and Rayleigh scattering contribution can influence the saturation effects encountered in forest SAR surveys and appear directly affected by growing dynamics within a forest. For the 3 simulated forest scenarios, R^2 values at P-Band of 0.45 for *Abies alba*, 0.96 for generic angiosperm, and 0.97 for the mixed species have been shown to represent a successful correlation between the simplistic model theory and the RT2 data. The low *Abies alba* result is possibly explained as a feature of forest overcrowding and uncertainties in boundaries assigned to Rayleigh size limits. For VHF the correlation is in general more reliable with *Abies alba* producing R^2 of 0.92, with generic angiosperm and mixed species giving values of 0.90 and 0.92 respectively. These are high values of correlation but generally lower than those presented at P-Band due to the increase in the proportion of Rayleigh scatterers when using longer wavelengths.

In natural climax forests, with major crown features, the contribution of these predominantly Rayleigh scatterers across the microwave range can be more significant than the negligible status they have been given in this study. Although it will be expected that their contribution will be to attenuate the signal, canopy scatterers will also be expected to increase the volume squared proportional backscatter quotient. Additional Rayleigh volume growth in the under-storey and canopy may also allow the backscatter of the forest to increase beyond the apparent saturation points, regardless of basal areas and may cause deviations from the theory. This is believed to be one reason why saturation may not be apparent. If a forest comprises an active canopy as well as regrowth on the forest floor then there will be a consistent Rayleigh presence which may grow and transition at a later point into the Optical regime. This is even true at very high SAR frequencies at which the sensitivity to scatterers in the upper layers of the forest is high. At low frequencies such as VHF the contribution of Rayleigh scattering will be prominent up to high volumes. This is due to the ratio of wavelength to radius, although the sensitivity to smaller scatterers will be low, resulting in lower relative intensity values than would be seen for a similar forest surveyed using a shorter wavelength. These trends are exhibited by backscatter estimates from both the simplistic model and the RT2 model.

6. Conclusions

We have demonstrated that a macroecological-based forest growth model can be used to drive a backscatter model based on the conceptual "Matchstick Model" (stems only) [8]. This has allowed a theoretical investigation into some of the trends associated with long wavelength radar and its relationship to stem growth within a forest environment. Significantly, the classic backscatter saturation-type curve is observed, even though scattering is confined to the effects of a single trunk layer. This provides significant further evidence that the stem structure, combined with structure-biomass dependence, is an additional driver of the backscatter-biomass curve, rather than being driven purely by the more typical opacity-based explanation. The simplistic model, similar to the Matchstick Model, was applied to demonstrate that backscatter trends can be explained to some extent by the transition from Rayleigh to Optical scattering signified by the change in size of the stems within a multi-age forest. A study of the coefficients of determination associated with the correlation between theoretical

backscatter values using the simplistic structural model (based on relationship with basal area and volume) and RT2 modelled backscatter has produced significant results. Over a 100 year period, starting from an initial planting density at year 0 of 25,000 stems, R^2 values >0.90 were reported for VHF band data for three forest structural scenarios; *Abies Alba*, Angiosperm, and Mixed Species (0.92, 0.90, 0.92 respectively). For P-Band data even higher R^2 values (>0.95) were reported for the Angiosperm and Mixed Forest scenarios (0.96, and 0.97 respectively) although a much lower value (0.45) was reported for the *Abies Alba* scenario at this frequency. This was interpreted as a feature of forest overcrowding and the inherent uncertainties in radius boundaries assigned to Rayleigh size limits. The results of this study have provided statistically significant ($p < 0.05$) modelling evidence to suggest that forest SAR backscatter behaviour at long microwave wavelengths can be described using two equations related to total stem volume and basal area, when Rayleigh and Optical scatterers dominate respectively. This is shown through the direct comparison of the modelled forest and the RT2 generated backscatter data. Furthermore, and most significantly, they serve to predict saturation like behaviour in the absence of canopy attenuation. This provides a significant source for future discussion and refinement with regard to biomass retrieval using radar backscatter. This is particularly apt with regard to proposed SAR missions chosen to provide such forest biomass measurements incorporating backscatter as a primary tool.

Each of the scenarios addressed in this work point to a relationship between stem size, and distribution within the forest, and the resultant backscatter. When total basal area remains consistent only small changes in backscatter are noted, even in the presence of multi-age and multi-sized stems, with varying backscatter levels assumed to result from the effects of senescence of larger trees (backscatter reduction) and forest regrowth (backscatter increase). The data provided in this study is largely dependent on the double bounce, stem to ground scattering which is considered a dominant scattering mechanism at long wavelengths [17] and is considered to be significantly influenced by the basal area of the forest. When this is not the case, such as when a forest over expands in basal area, attenuation of the important double bounce scattering is more likely to be responsible. As the RT2 model used to generate backscatter is an incoherent model, the significance of this double bounce is reduced within the modelled data.

Although the impact of attenuation on the backscatter-biomass curve is not debated, and has been shown to be active in this study, its role in saturating the backscatter is at least matched by the existence of structural trends that survive even in the absence of attenuating influences. In the SERA model, as the forest increases in volume and age, the number density of stems consistently decrease to further reduce the impact of occlusion. This impact is seen in both the simplistic model and the RT2 model backscatter data, which are both shown to correlate well with the forest data.

To complement this work, studies including canopy elements would be beneficial, butmay also reduce benefits gained from using the simple model. Canopy elements would enable further analysis of the Rayleigh influence on these saturation events to determine whether their presence can alter the limit of saturation, or prevent it indefinitely. In addition, the contribution of secondary branches likely to provide a large Optical scattering element could be assessed as they could significantly increase the intensity of the direct backscatter. This study remains a modelling investigation relying heavily on the predictions of the models used and, as such, the results are for a simplified scenario where the emphasis is on trends, rather than absolute values. Even so, the trends are confidently presented as many

assumptions made in this study align with published scattering behaviour, particularly at long wavelengths.

Acknowledgments

Author Contributions

Matthew Brolly was responsible for defining concept, conducting experimental procedures and the writing of this work. Iain H. Woodhouse was instrumental in developing key concepts and ideas whilst also contributing to the editing process.

Conflicts of Interest

The authors declare no conflict of interest.

Reference

1. Attema, E.P.W.; Ulaby, F.T. Vegetation modeled as a water cloud. *Radio Sci.* **1978**, *13*, 357–364.
2. Papathanassiou, K.P.; Cloude, S.R. Single-Baseline polarimetric SAR interferometry. *IEEE Trans. Geosci. Remote Sens.* **2002**, *39*, 2352–2363.
3. Woodhouse, I.H. Predicting backscatter-biomass and height-biomass trends using a macroecology model. *IEEE Trans. Geosci. Remote Sens.* **2006**, *44*, 871–877.
4. Santos, J.; Lacruz, M.S.P.; Araujo, L.; Keil, M. Savanna and tropical rainforest biomass estimation and spatialization using JERS-1 data. *Int. J. Remote Sens.* **2002**, *23*, 1217–1229.
5. Fransson, J.E.S.; Israelsson, H. Estimation of stem volume in boreal forests using ERS-1 C-and JERS-1 L-band SAR data. *Int. J. Remote Sens.* **1999**, *20*, 123–137.
6. Smith, G.; Ulander, L.M.H. A model relating VHF-band backscatter to stem volume of coniferous boreal forest. *IEEE Trans. Geosci. Remote Sens.* **2000**, *38*, 728–740.
7. Smith-Jonforsen, G.; Folkesson, K.; Hallberg, B.; Ulander, L.M.H. Effects of forest biomass and stand consolidation on p-band backscatter. *IEEE Geosci. Remote Sens. Lett.* **2007**, *4*, 669–673.
8. Brolly, M.; Woodhouse, I.H. A "Matchstick Model" of microwave backscatter from a forest. *Ecol. Modell.* **2012**, *237–238*, 74–87.
9. West, G.B.; Brown, J.H.; Enquist, B.J. A General model for the origin of allometric scaling laws in biology. *Science* **1997**, *276*, doi:10.1126/science.276.5309.122.
10. Brolly, M.; Woodhouse, I.H. Vertical backscatter profile of forests predicted by a macroecological plant model. *Int. J. Remote Sens.* **2013**, *34*, 1026–1040.
11. Brolly, M.; Woodhouse, I.H.; Niklas, K.J.; Hammond, S.T. A macroecological analysis of SERA derived forest heights and implications for forest volume remote sensing. *PLoS One* **2012**, *7*, doi:10.1371/journal.pone.0033927.

12. Hammond, S.T.; Niklas, K.J. Emergent properties of plants competing in silico for space and light: Seeing the tree from the forest. *Am. J. Bot.* **2009**, *96*, 1430–1440.

13. Cookmartin, G.; Saich, P.; Quegan, S.; Cordey, R.; Burgess-Allen, P.; Sowter, A. Modeling microwave interactions with crops and comparison with ERS-2 SAR observations. *IEEE Trans. Geosci. Remote Sens.* **2000**, *38*, 658–670.

14. Balzter, H.; Skinner, L.; Luckman, A.; Brooke, R. Estimation of tree growth in a conifer plantation over 19 years from multi-satellite L-band SAR. *Remote Sens. Environ.* **2003**, *84*, 184–191.

15. Crispin, J.W.; Maffett, A.L. Radar cross-section estimation for simple shapes. *IEEE Proc.* **1965**, *53*, 833–848.

16. Cloude, S.R.; Pottier, E. An entropy based classification scheme for land applications of polarimetric SAR. *IEEE Trans. Geosci. Remote Sens.* **1997**, *35*, 68–78.

17. Saatchi, S.S.; McDonald, K.C. Coherent effects in microwave backscattering models for forest canopies. *IEEE Trans. Geosci. Remote Sens.* **1997**, *35*, 1032–1044.

18. Enquist, B.J.; Brown, J.H.; West, G.B. Allometric scaling of plant energetics and population density. *Nature* **1998**, *395*, 163–165.

19. Niklas, K.J. Modeling fossil plant form-function relationships: A critique. *Paleobiology* **2000**, *26*, 289–304.

20. Chave, J. Study of structural, successional and spatial patterns in tropical rain forests using TROLL, a spatially explicit forest model. *Ecol. Modell.* **1999**, *124*, 233–254.

21. Moorcroft, P.R.; Hurtt, G.C.; Pacal, S.W. A method for scaling vegetation dynamics: The ecosystem demography model (ED). *Ecol. Monogr.* **2001**, *71*, 557–586.

22. Ulander, L.M.H.; Askne, J.; Fransson, J.; Gustavsson, A.; le Toan, T.; Manninen, T.; Martinez, J.M.; Melon, P.; Smith, G.; Walter, F. Retrieval of stem volume in coniferous forest from low VHF-band SAR. In Proceedings of the Geoscience and Remote Sensing Symposium, IGARSS 2000, Honolulu, HI, USA, 24–28 July 2000; pp. 441–443.

23. Dobson, M.C.; Ulaby, F.T.; LeToan, T.; Beaudoin, A.; Kasischke, E.S.; Christensen, N. Dependence of radar backscatter on coniferous forest biomass. *IEEE Trans. Geosci. Remote Sens.* **1992**, *30*, 412–415.

24. Moghaddam, M.; Saatchi, S. Analysis of scattering mechanisms in SAR imagery over boreal forest: Results from BOREAS'93. *IEEE Trans. Geosci. Remote Sens.* **1995**, *33*, 1290–1296.

25. Studies of Phase Center and Extinction Coefficient for Boreal Forest Using X-And L-Band Polarimetric Interferometry Combined with Lidar Measurement. Available online: http://earth.esa.int/workshops/polinsar2009/participants/365/paper_365_p4-6prak.pdf (accessed on 22 July 2014).

26. Papathanassiou, K.P.; Kugler, F.; Lee, S.; Marotti, L.; Hajnsek, I. Recent advances in polarimetric SAR interferometry for forest parameter estimation. In Proceedings of the Radar Conference, 2008. RADAR '08, Rome, Italy, 26–20 May 2008; pp. 1–6.

27. Gifford, E.M.; Foster, A.S. *Morphology and Evolution of Vascular Plants*; WH Freeman and Co.: New York, NY, USA, 1989.

28. Taiz, L.; Zeiger, E. *Plant Physiology*, 3rd ed.; Sinauer Associates, Inc.: Sunderland, UK, 2002.

29. Marbà, N.; Duarte, C.M.; Agustí, S. Allometric scaling of plant life history. *Proc. Natl. Acad. Sci. USA* **2007**, *104*, 15777–15780.

30. Niklas, K.J.; Spatz, H.C. Growth and hydraulic (not mechanical) constraints govern the scaling of tree height and mass. *Proc. Natl. Acad. Sci. USA* **2004**, *101*, 15661–15663.

31. Cannell, M.G.R. *World Forest Biomass and Primary Production Data*; Academic Press: New York, NY, USA, 1982.

32. Moosmuller, H.; Arnott, P. Particle optics in the Rayleigh regime. *J. Air Waste Manag. Assoc.* **2009**, *59*, 1028–1031.

33. Lopes, A.; Mougin, E.; Beaudoin, A.; Karam, M.A. Relating the microwave signatures of trees to their structure results of an experimental/theoretical approach. *IEEE Trans. Geosci. Remote Sens.* **1991**, *29*, 344–365.

34. Mougin, E.; Lopes, A.; Karam, M.A.; Fung, A.K. Effect of tree structure on X-band microwave signature ofconifers. *IEEE Trans. Geosci. Remote Sens.* **1993**, *31*, 655–667.

35. Woodhouse, I.H. *Introduction to Microwave Remote Sensing*; CRC Press, Taylor & Francis Group: Boca Raton, FL, USA, 2006.

36. Hestilow, T.J. Simple formulas for the calculation of the average physical optics RCS of a cylinder and a flat plate over a symmetric window around broadside. *IEEE Antennas Propag. Mag.* **2000**, *42*, 48–52.

37. Ulaby, F.T.; Sarabandi, K.; McDonald, M.; Whitt, M.; Dobson, M.C. *Michigan Microwave Canopy Scattering Model* (*MIMICS*); The University of Michigan: Ann Arbor, MI, USA, 1988; Tech. Rep. 022486-T-1.

38. Imhoff, M.L. A theoretical analysis of the effect of forest structure on synthetic aperture radar backscatter and the remote sensing of biomass. *IEEE Trans. Geosci. Remote Sens.* **1995**, *33*, 341–352.

39. Woodhouse, I.H.; Hoekman, D.H. Radar modelling of coniferous forest using a tree growth model. *Int. J. Remote Sens.* **2000**, *21*, 1725–1737.

40. Ferrazzoli, S.; Paloscia, P.; Pampaloni, G.; Schiavon, S.; Sigismondi, S.; Solimini, D. The potential of multifrequency polarimetric SAR is assessing agricultural and arboreous biomass. *IEEE Trans. Geosci. Remote Sens.* **1997**, *35*, 5–17.

41. Ranson, K.J.; Sun, G. Mapping biomass of a northern forest using multifrequency SAR data. *IEEE Trans. Geosci. Remote Sens.* **1994**, *32*, 388–396.

42. Schiavon, G.; Solimini, D.; Burini, A. Sensitivity of multi-temporal high resolution polarimetric C and L-band SAR to grapes in vineyards. In Proceedings of the Geoscience and Remote Sensing Symposium, 2007. IGARSS 2007, Barcelona, Spain, 23–28 July 2007, pp. 3651–3654.

43. Ulaby, F.T.; Moore, R.K.; Fung, A.K. *Microwave Remote Sensing, Active and Passive, Volume II: Radar Remote Sensing and Surface Scattering and Emission Theory*; Addison-Wesley Publishing Co: Boston, MD, USA, 1982; Chapter 11.

44. Le Toan, T.; Quegan, S.; Davidson, M.; Balzter, H.; Paillou, P.; Papathanassiou, K.; Plummer, S.; Rocca, F.; Saatchi, S.; Shugart, H. The biomass mission: Mapping global forest biomass to better understand the terrestrial carbon cycle. *Remote Sens. Environ.* **2011**, *115*, 2850–2860.

45. Dubois-Fernandez, P.; Champion, P.I.; Guyon, D.; Cantalloube, H.; Garestier, F.; Dupuis, X. Forest biomass estimation from P-band high incidence angle data. In Proceedings of the PolInSAR Workshop, ESA, ESRIN, Frascati, Italy, 17–21 January 2005.

46. Tang, K.; Dimenna, R.A.; Buckius, R.O. Regions of validity of the geometric optics approximation for angular scattering from very rough surfaces. *Int. J. Heat Mass Transfer* **1996**, *40*, 49–59.

47. Hallikainen, M.T.; Ulaby, F.T.; Dobson, M.C.; El-Rayes, M.A.; Wu, L.K. Microwave dielectric behavior of wet soil-Part I: Empirical models and Experimental observations. *IEEE Trans. Geosci. Remote Sens.* **1985**, *GE-23*, 25–34.

48. Ulaby, F.T.; El-Rayes, M.A. Microwave dielectric spectrum of vegetation Part II: Dual dispersion model. *IEEE Trans. Geosci. Remote Sens.* **1987**, *325*, 550–557.

49. Baker, J.R.; Mitchell, P.L.; Cordey, R.A.; Groom, G.B.; Settle, J.J.; Stileman, M.R. Relationships between physical characteristics and polarimetric radar backscatter for Corsican pine stands in Thetford Forest, UK. *Int. J. Remote Sens.* **1994**, *15*, 2827–2849.

50. Imhoff, M.L. Radar backscatter and biomass saturation: Ramifications for global biomass inventory. *IEEE Trans. Geosci. Remote Sens.* **1995**, *33*, 511–518.

51. Shvidenko, A.; Venevsky, S.; Nilsson, S. *Increment and Mortality for Major Forest Species of Northern Eurasia with Variable Growing Stock*; International Institute for Applied Systems Analysis: Laxenburg, Austria, 1996.

52. Patenaude, G. *Remote Sensing and LULUCF Carbon Inventories in the UK, DEFRA, 2003. UK Emissions by Sources and Removals by Sinks due to Land Use, Land Use Change and Forestry Activities*; Department for the Environment, Food and Rural Affairs (DEFRA): London, UK, 2003; pp. 1–59.